Ozone loss driven by nitrogen oxides and triggered by stratospheric warmings can outweigh the effect of halogens

Paul Konopka,[1] Andreas Engel,[2] Bernd Funke,[3] Rolf Müller,[1] Jens-Uwe Grooß,[1] Gebhard Günther,[1] Thomas Wetter,[2] Gabriele Stiller,[4] Thomas von Clarmann,[4] Norbert Glatthor,[4] Hermann Oelhaf,[4] Gerald Wetzel,[4] Manuel López-Puertas,[3] Michel Pirre,[5] Nathalie Huret,[5] and Martin Riese[1]

Received 9 January 2006; revised 9 October 2006; accepted 2 November 2006; published 3 March 2007.

[1] Ozone loss in the lower and middle stratosphere in spring and summer, in particular over polar regions, is driven mainly by halogens and nitrogen oxides (NO_x). Whereas the stratospheric chlorine levels are expected to decrease in the future, the role of NO_x for the O_3 budget in a changing climate is not well quantified. Here we combine satellite measurements and model simulations to diagnose the accumulated O_3 loss during winter and spring 2002–2003 in the Arctic polar stratosphere. We show that in a winter stratosphere strongly disturbed by warmings, O_3 loss processes driven by halogens and NO_x can significantly overlap within the polar column and become comparable in magnitude even if a significant, halogen-induced O_3 loss has occurred. Whereas, until the beginning of March 2003, polar column O_3 loss was mainly caused by the halogen chemistry within the vortex at an altitude around 18 km, the chemical O_3 destruction in March and April was dominated by the NO_x chemistry in O_3-rich air masses transported from the subtropics and mixed with the polar air above the region affected by the halogens. This NO_x-related O_3 loss started around mid-December 2002 in subtropical air masses above 30 km that moved poleward after the major warming in January, descended to 22 km with an increasing magnitude of O_3 loss and reached surprisingly high values of up to 50% local loss around the end of April. To some extent, the NO_x-driven O_3 loss was enhanced by mesospheric air trapped in the vortex at the beginning of the winter as a layer of few km in the vertical and transported downward within the vortex. The effect of NO_x transported from the subtropics dominated the O_3 loss processes in the polar stratosphere in spring 2003, both relative to the effect of the halogens and relative to the contribution of the mesospheric NO_x sources. A comparison with the 1999/2000 Arctic winter and with the Antarctic vortex split event in 2002 shows that wave events triggered by stratospheric warmings may significantly enhance O_3 loss driven by NO_x when O_3- and NO_x-rich air masses from the subtropics are transported poleward and are mixed with the vortex air.

Citation: Konopka, P., et al. (2007), Ozone loss driven by nitrogen oxides and triggered by stratospheric warmings can outweigh the effect of halogens, *J. Geophys. Res.*, *112*, D05105, doi:10.1029/2006JD007064.

1. Introduction

[2] In the past two decades, O_3 loss in the polar lower stratosphere in winter and early spring has been inferred from a great variety of measurements and, to a large extent, could be explained in terms of halogen-induced O_3 destruction processes [e.g., *Solomon*, 1999; *Harris et al.*, 2002; *Manney et al.*, 2003; *Tilmes et al.*, 2004; *World Meteorological Organization* (*WMO*), 2003]. On the other hand, there are also natural chemical processes controlling stratospheric O_3 mainly driven by photochemical cycles involving nitrogen and hydrogen oxides (NO_x, HO_x) [*Brasseur and Solomon*, 1984].

[3] It is well known that during polar summer, NO_x chemistry is an effective photolytical mechanism destroying O_3 in the stratosphere [*Farman*, 1985; *Perliski et al.*, 1989]. Typically, this O_3 decline begins when the stratosphere undergoes a transition in late spring, from a circulation dominated by the polar vortex, sometimes affected by

[1]ICG-I: Stratosphäre, Forschungszentrum Jülich, Jülich, Germany.
[2]Institut für Meteorologie und Geophysik, Johann Wolfgang Goethe-Universität Frankfurt, Frankfurt am Main, Germany.
[3]Instituto de Astrofisica de Andalucia, Consejo Superior de Investigaciones Cientficas, Granada, Spain.
[4]Institut für Meteorologie und Klimaforschung, Forschungszentrum Karlsruhe, Karlsruhe, Germany.
[5]Laboratoire de Physique et Chemie de l'Environnement, Orleans, France.

0148-0227/07/2006JD007064

planetary waves, to a weakly disturbed circumpolar rotation in summer [*Newman et al.*, 1999; *Fahey and Ravishankara*, 1999].

[4] *Manney et al.* [1994] discussed a significant O_3 loss in air masses transported during stratospheric warmings from the low latitudes into the polar middle stratosphere and trapped as so-called low-O_3 pockets in the stationary anticyclones over the polar regions. The primary mechanism responsible for the development of these low-O_3 regions is the isolation of air in such anticyclones for periods of time long enough to destroy O_3 (mainly because of NO_x) by adjusting its mixing ratio to a new local equilibrium [*Morris et al.*, 1998]. O_3 loss induced by NO_x also occurs in the autumn polar stratosphere [*Kawa et al.*, 2002].

[5] The stratospheric NO_x and HO_x radicals are primarily of natural origin although anthropogenic emissions do contribute to the atmospheric loading of N_2O and CH_4, which are sources of NO_x and HO_x [e.g., *WMO*, 2003]. The regions with the highest production of NO_x are located in the tropical stratosphere around 40 km (i.e., above the O_3 maximum at $\approx$30 km) and in the polar mesosphere. The latter occurs episodically and is caused by solar flares with associated energetic particle precipitation followed by downward transport into the polar vortex [e.g., *Siskind et al.*, 2000; *Natarajan et al.*, 2004; *López-Puertas et al.*, 2005; *von Clarmann et al.*, 2005].

[6] Since NO_x drives the main catalytic loss cycle of O_3 in the midstratosphere, variations in NO_x significantly contribute to global O_3 variability. Further, the relative contributions of NO_x- and halogen-induced O_3 loss processes to the observed negative decadal trends in the total column of O_3 in midlatitudes, and even in the polar regions, are not well quantified [*WMO*, 2003].

[7] It is also generally accepted that the polar O_3 loss triggered by halogens mainly occurs in late winter and spring within the polar vortex and that the NO_x-induced O_3 destruction roughly follows the halogen chemistry, after the vortex breakup in late spring and summer with highest values occurring in the middle and lower stratosphere. The main focus of this paper is to show that if the winter stratosphere is strongly disturbed by warmings, these two catalytic cycles can significantly overlap, both in time and space (i.e., both effects destroy O_3 within the polar column during the winter). Their effect on column O_3 becomes comparable in magnitude even if a significant, halogen-induced O_3 loss has occurred.

[8] In the following, we analyze the O_3 loss over the course of winter and spring 2002–2003, i.e., a winter that was significantly influenced by the major warming in January 2003 triggering a rapid transport of O_3- and NO_x-rich air masses from the subtropics to the Arctic [*Kleinböhl et al.*, 2005]. In addition, we discuss the relevance of the mesospheric air observed during 3 balloon flights inside the vortex in January and March 2003 [*Engel et al.*, 2006] to O_3 loss. To understand how representative our results are, we also apply our diagnostics of O_3 loss for a typical, undisturbed cold Arctic winter such as 1999–2000 and for the highly disturbed Southern Hemispheric winter 2002 when an unprecedented major stratospheric warming in late September split the polar vortex into two parts. Finally, we discuss how increased poleward transport, as predicted for the future climate, may influence the O_3 budget in the high latitudes and midlatitudes.

2. Ozone Loss in Winter and Spring 2002–2003

2.1. Satellite Observations and Simulations With CLaMS

[9] To diagnose the accumulated O_3 loss in the middle and lower polar stratosphere we use satellite observations of O_3 from the POAM (Polar Ozone and Aerosol Measurement III) [*Lucke et al.*, 1999; *Lumpe et al.*, 2002] and MIPAS (Michelson Interferometer for Passive Atmospheric Sounding) instruments [*European Space Agency*, 2000]. In addition, vertical profiles of O_3, CH_4, CO, and NO_x (NO_x = NO + NO_2) generated by the Institute for Meteorology and Climate Research and the Instituto de Astrofiacute;sica de Andalucia (IMK-IAA-MIPAS) were used (version V1_*_2, where * means a given species). The data analysis of O_3 and CH_4 is reported by *Glatthor et al.* [2004] and the retrievals of CO and NO_x are documented by *Funke et al.* [2004].

[10] The accumulated ozone loss ΔO_3 is derived from the difference between the observed and the so-called passive O_3 (pO_3, i.e., O_3 passively transported without any chemistry) calculated with the Chemical Lagrangian Model of the Stratosphere (CLaMS) [*McKenna et al.*, 2002; *Konopka et al.*, 2004]. To provide reliable spatial distributions of pO_3, high-resolution CLaMS studies of passively transported O_3 and CH_4 were carried out with air parcels (APs) covering the Northern Hemisphere in the altitude range between 15 and 45 km corresponding to the potential temperature (θ) range between 350 and 1400 K. The mean horizontal separation between the APs is given by 50 km and 100 km poleward and equatorward of 30°N, respectively. The mean vertical separation between the APs results from a prescribed constant aspect ratio α = 250 (describing the ratio between the resolved horizontal and vertical scales) and is given by 200 and 500 m in the high- and low-resolution regime, respectively.

[11] The model was initialized on 17 November 2002, i.e., before the onset of polar stratospheric cloud (PSC) formation [*Tilmes et al.*, 2003]. The initialization of CH_4 (using equivalent latitude mapping of HALOE observations) and O_3 (by gridding of the near-real-time ESA-MIPAS data) is described in [*Grooß et al.*, 2005]. To quantify the dilution of the vortex air due to intrusions of the midlatitude air into the vortex, an artificial tracer is transported in CLaMS that, at the beginning of the simulation, marks the APs inside and outside the vortex as 100% and 0%, respectively, with the vortex edge defined by the *Nash et al.* [1996] criterion (maximum of isentropic PV gradient with respect to the equivalent latitude as derived from ECMWF data). Thus the vortex tracer that undergoes mixing over the course of the model run describes the percentage of original vortex air in each AP.

[12] The top and bottom boundary conditions for CH_4 and O_3 at 1400 and 350 K are updated every 24 hours on the basis of the MIPAS observations (top) and by using the HALOE climatology (bottom) [*Grooß and Russell*, 2005]. We use O_3 from MIPAS instead of POAM observations because of better coverage of the entire Northern Hemisphere. The impact of the upper boundary on the tracer distribution within the model domain propagates down-

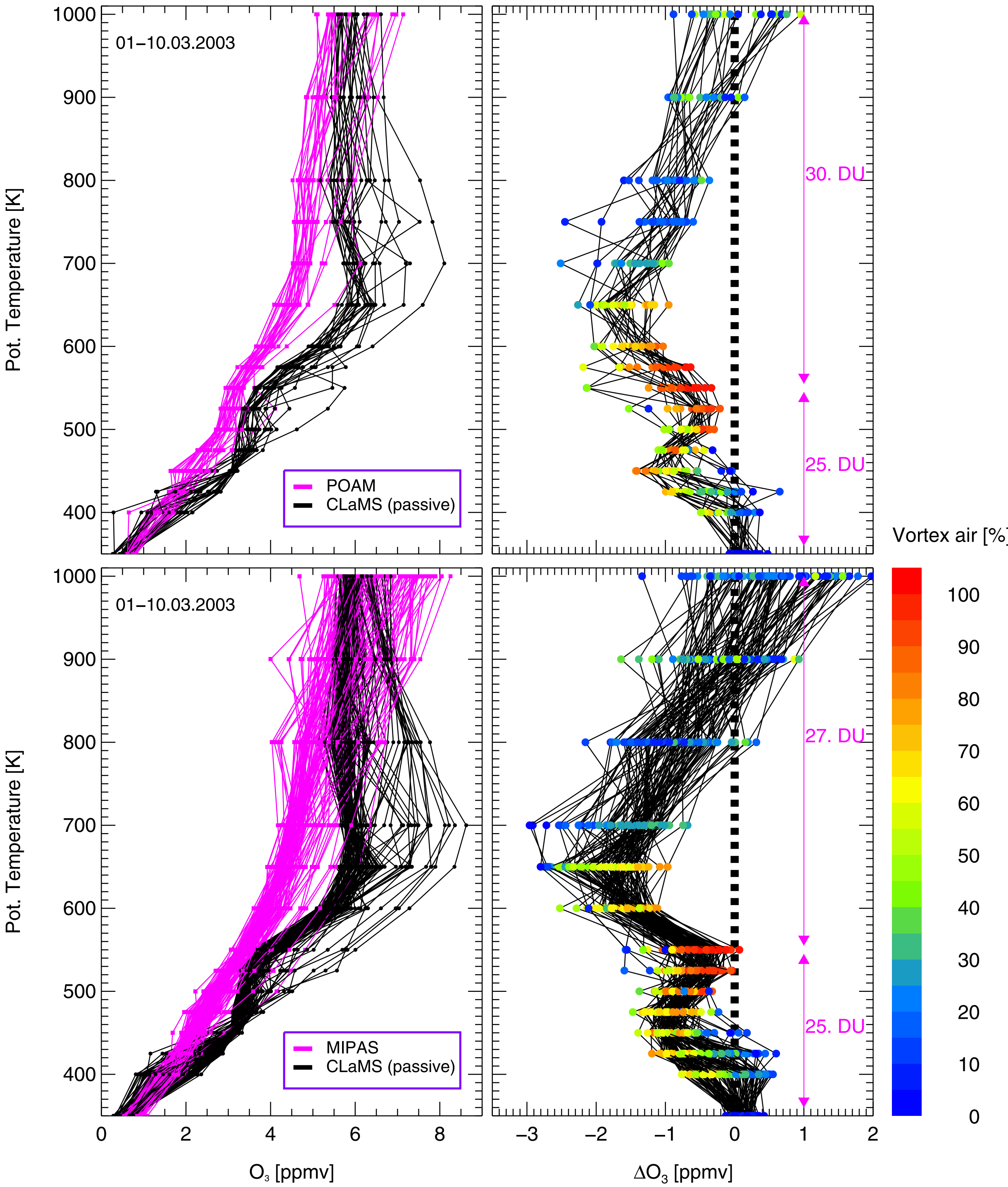

Figure 1. (left) O_3 profiles observed (pink) by (top) POAM and (bottom) MIPAS versus passive O_3 transported by CLaMS (black) between 1 and 10 March and poleward of 65°N equivalent latitude (calculated at $\theta = 450$ K). (right) Corresponding O_3 loss (ΔO_3), i.e., the difference between the observed and simulated profiles. Each air parcel sampled along the profile (bold circles) was colored by the percentage of the pure vortex air calculated with CLaMS (i.e., red means air masses within a well-isolated vortex). The pink arrows denote the column O_3 loss integrated between 350–550 K and 550–1000 K which, as shown in this paper, can be attributed to halogen and NO_x chemistry, respectively.

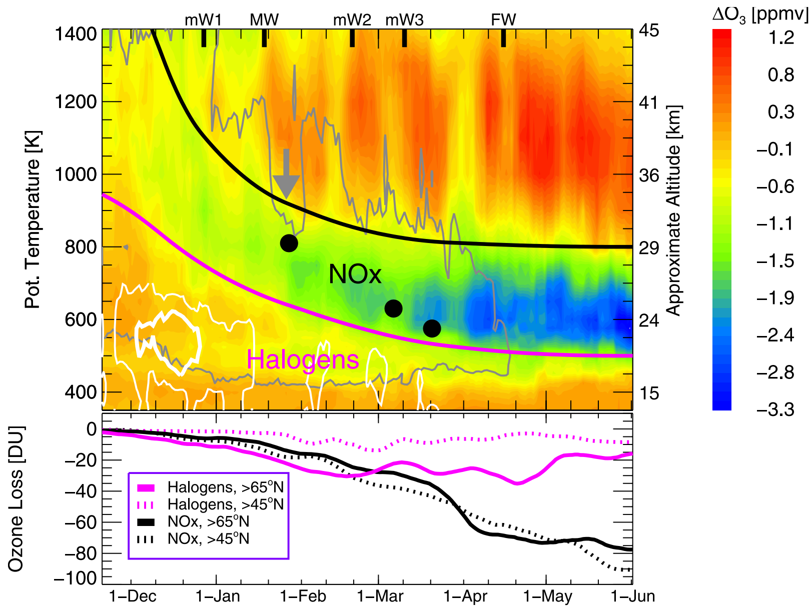

Figure 2. (top) Accumulated O_3 loss (ΔO_3) between 17 November 2002 and 1 June 2003 and averaged poleward of 65°N equivalent latitude (calculated at θ = 450 K). ΔO_3 is derived from the difference between the satellite observations (POAM) and simulated passive O_3 (CLaMS). A well-isolated vortex exists within the gray line. As a consequence of the major warming (MW) in January, an increase of the vortex permeability (gray arrow) leads to a strong intrusion of subtropical, O_3-rich air into the polar region. The black dots denote places where balloons sampled mesospheric air. The thick pink line approximates the upper boundary of the region where PSCs were observed (thin and thick white lines correspond to the possible PSC area of 1 and 10 $\times$ 10^6 km^2, respectively [*Tilmes et al.*, 2003]). The thick black line approximately separates the region of O_3 loss from the region of O_3 production. (bottom) Corresponding column O_3 loss (solid lines) calculated below the thick pink line (halogen-induced within the vortex) and between the thick black and pink lines (NO_x-induced). The dotted lines result when our calculations are extended over a region poleward of 45°N equivalent latitude (MIPAS).

ward, mainly within the polar vortex, to about 800 K at the beginning of April. Transport in CLaMS was validated by comparing simulated distributions of CH_4 for winter 2002–2003 with in situ measurements on board the Geophysica research aircraft and balloon platforms as well as with HALOE observations (correlation coefficient higher than 0.97 [*Grooß and Russell*, 2005]). The quality of pO_3 was ensured by comparison with MIPAS and POAM O_3 observations during the first 4 weeks of transport (i.e., during the time when mixing ratios were not disturbed by subtropical intrusions) which show no biases and the correlation coefficients are higher than 0.96.

2.2. Ozone Loss in the Arctic Stratosphere

[13] An example of how the chemical O_3 loss, ΔO_3, can be inferred from the difference between the passive (CLaMS) and observed (POAM, MIPAS) O_3 is shown in Figure 1, where in the left column the O_3 profiles measured (pink) by the POAM (top) and MIPAS (bottom) instruments between 1 and 10 March are compared with pO_3 interpolated from the nearest CLaMS APs to the location of the measurement (black). To compare ΔO_3 caused by the halogen-induced chemistry within the vortex with other, column-relevant, mainly NO_x-driven processes above the vortex, we consider only profiles intercepting the potential temperature surface θ = 450 K at geographic locations with equivalent latitude >65°N. Since the highest halogen-induced ΔO_3 was observed at 450 K during this winter [*Grooß et al.*, 2005], we are thus able to quantify the impact of different ozone destroying processes in relation to the well-known effect of halogen chemistry within the polar vortex.

[14] Thus, in the right-hand column of Figure 1, the corresponding profiles of ΔO_3 are derived where two characteristic maxima, around 450 and 700 K, and a minimum around 550 K, are apparent. The colors of the filled circles denote the calculated (CLaMS) percentage of the vortex air in the sampled air masses starting from 17 November 2002. Values above 50%, with the highest values between 500 and 550 K, indicate a well-isolated vortex. The corresponding values of O_3 loss integrated over altitude (column O_3 loss, negative/positive values mean O_3 loss/production) between 350–550 K and 550–1000 K are of similar magnitude with values of 25 and 27 (MIPAS)/30 (POAM) DU, respectively. Whereas O_3 loss around 450 K mainly occurs in air masses within the vortex (vortex air percentage larger than 50%), ΔO_3 above 550 K is only moderately influenced by the vortex air.

[15] To derive the time evolution of O_3 loss in high latitudes, we extend this procedure to the period from 17 November 2002 to 1 June 2003. Figure 2 shows the time dependence of the accumulated ΔO_3 calculated by subtracting CLaMS pO_3 from the POAM O_3 observations and averaging over time (3-day running mean) and in each

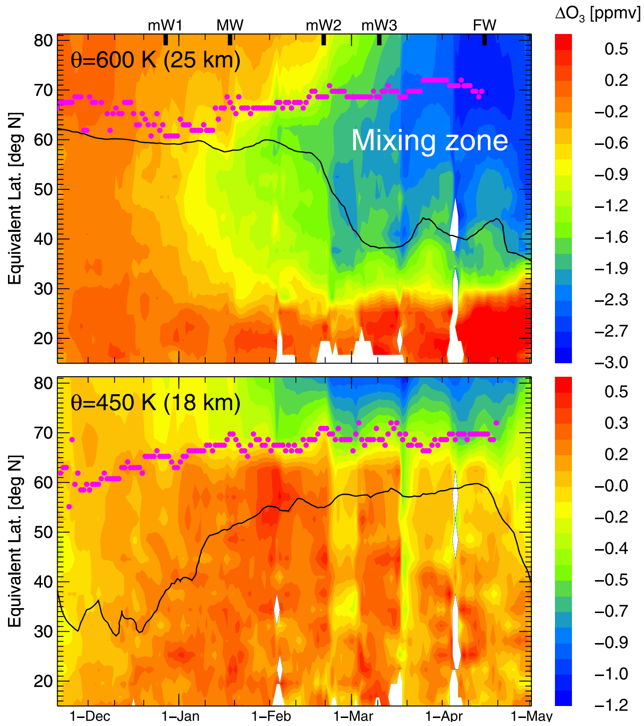

Figure 3. Horizontal (isentropic) view of the NO_x-induced ΔO_3 at $\theta = 600$ (top) and halogen-induced ΔO_3 at $\theta = 450$ K (bottom). O_3 loss is derived from the difference between the MIPAS observations and CLaMS passive O_3. Pink dots denote the vortex edge. The black line describes the vortex isolation, i.e., according to CLaMS, poleward of this line the air masses contain more than 5% vortex air. Thus the region between the vortex edge and this line can be understood as the mixing zone between the vortex and extra vortex air. In white regions no MIPAS profiles were available. Some of the vertical stripes are artificial because of insufficient statistics. Note that the contour levels are different in the top and bottom plots.

θ layer over all the profiles with equivalent latitude >65°N at the 450 K potential temperature surface. Using this criterion, we quantify ΔO_3 within the polar column containing that part of the vortex where the highest halogen-induced ozone loss was found [*Grooß et al.*, 2005]. Dates of occurrence of the minor (mW) major (MW) and final (FW) warmings are marked in Figure 2. The gray line shows the isoline of the MPV (modified PV, [*Lait*, 1994]) gradient with respect to the equivalent latitude calculated for 1.5 MPV units per degree of equivalent latitude. This value was empirically determined by *Steinhorst et al.* [2005] as a quantitative measure of the strength of the vortex edge and in particular of its permeability.

[16] Starting from the end of December (mW1), the vortex decayed from the top until the vortex breakup in late April 2003 with a strong increase of vortex permeability (gray arrow) and subsequent vortex dilution around 800 K (~30 km) triggered by the major warming (MW) in January. *Kleinböhl et al.* [2005] showed that during and after this warming, subtropical, O_3-rich air masses were transported into the Arctic stratosphere above a still intact and isolated vortex. During this period, the stratospheric dynamics was mainly disturbed by planetary waves with the zonal wave number 2 [*Kleinböhl et al.*, 2005].

[17] In the following, we will discuss ozone loss within two different air masses (branches). Whereas ΔO_3 within the first air mass is confined to the interior of the Arctic polar vortex below ≈600 K (lower branch), ΔO_3 within the second air mass mainly occurs in the region above ≈600 K during the transport from the subtropics to high latitudes (upper branch). The accumulated ΔO_3 poleward of 65°N shown in Figure 2 allows to distinguish between the contributions of these both branches.

[18] The lower, weaker branch in Figure 2 (below the pink line) coincides with an increased occurrence of PSCs (white contours) and can be attributed to the halogen chemistry in the vortex [see, e.g., *Feng et al.*, 2005; *Grooß et al.*, 2005]. The upper, more pronounced branch of ΔO_3 that is confined by the pink and black lines (black line approximately separates the region of O_3 loss from the region of O_3 production) is a result of O_3 loss with two different contributions: a (minor) contribution within the air that descended from above 1200 K (~40 km) in late November within the vortex and a (major) contribution that started around mid-December 2002 in a wide tongue of subtropical air masses at ~30 km.

[19] The signature of ΔO_3 within this subtropical intrusion moved poleward after the major warming in January and descended to 22 km with significantly increased magnitude around the end of March. On the basis of the IMK-IAA-MIPAS observations of all relevant nitrogen components (NO_y), the air masses of subtropical origin are characterized by high values of NO_y (between 10 and 20 ppbv, not shown) and, consequently, the O_3 loss in these air masses is likely to be driven by NO_x catalytic cycles, a conclusion that is also supported by model studies [*Singleton et al.*, 2005; *Grooß et al.*, 2005]. Thus, in agreement with the general understanding of the stratospheric chemistry, we assign the lower and upper branches of ΔO_3 in Figure 2 to the halogen and NO_x-induced processes, respectively. The latter one includes also the HO_x chemistry, as our box model calculations suggest (section 5), the contribution of HO_x is of the order of 10%.

[20] The corresponding mean column O_3 loss is shown in Figure 2 (bottom) where the thick pink and black lines quantify the halogen- and the NO_x-induced contribution, respectively. The halogen-induced contribution is derived from the column O_3 loss below the pink line in Figure 2 (top) (i.e., mainly caused by the chemistry within the vortex) and the NO_x-induced O_3 loss describes the contribution of the column loss between the black and pink lines (i.e., from depletion processes in the mixing zone above the most stable part of the vortex).

[21] Thus, even though the contribution of the O_3 loss within the vortex is the most important factor for chemical O_3 loss until the end of February (≈40 DU), in March and April the NO_x-induced O_3 depletion in the decaying upper part of the vortex dominates the column O_3 loss with values of 80 DU (i.e., more than twice the O_3 loss due to the halogen contribution) shortly before the final warming. Because the density of air strongly decreases with the altitude, the derived mean column O_3 loss only weakly depends on the exact position of the black line (±5 DU by

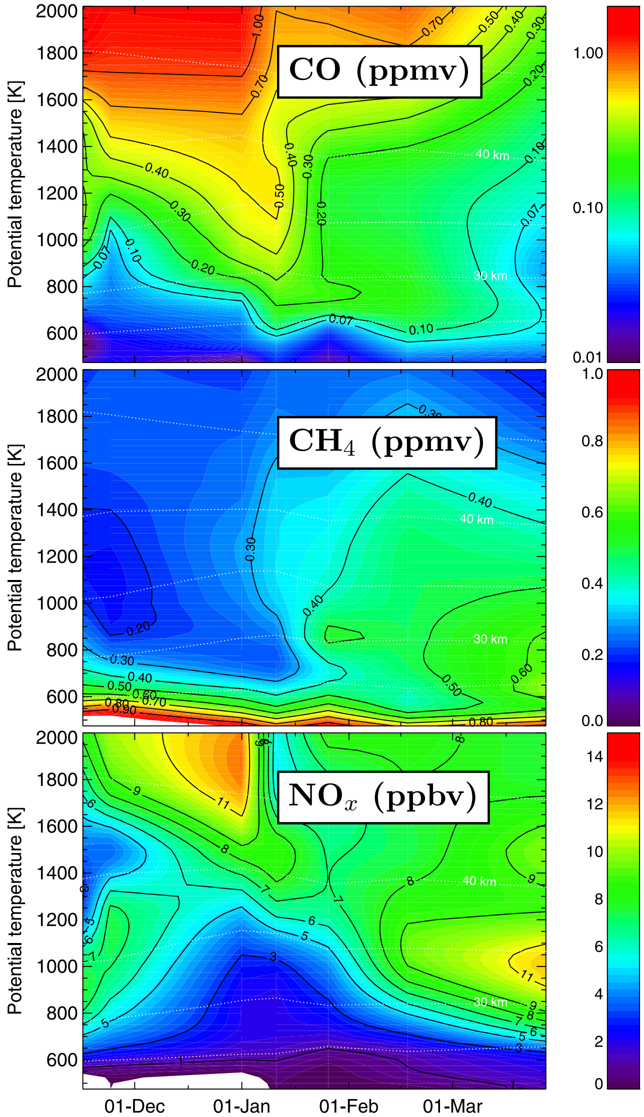

Figure 4. IMK-IAA-MIPAS satellite observations of (top) CO, (middle) CH_4 and (bottom) NO_x. The observed profiles are averaged poleward of 70°N equivalent latitude and are shown in the potential temperature range between 475 and 2000 K. For CO a logarithmic color scale was used. The mesospheric tracer (CO) and the extra vortex tracer (CH_4) allow us to assign the sources of NO_x which caused the reported O_3 loss in the polar stratosphere.

shifting the black line by ±100 K up and downward, respectively).

2.3. Impact of Meridional Transport on Polar Ozone Loss

[22] To localize the meridional distribution of O_3 loss more precisely, in Figure 3 we now discuss both branches of ΔO_3 at two horizontal (isentropic) surfaces 450 K (~18 km) and 600 K (~25 km). Whereas the halogen-induced O_3 loss is strongly confined to the interior of the vortex (Figure 3, bottom) with the vortex edge denoted by the pink dots [*Nash et al.*, 1996], the signature of the NO_x-induced O_3 loss starts in January outside the vortex (Figure 3, top).

[23] Although the earliest evidence of the NO_x branch arises within the vortex above 1200 K (~40 km) (Figure 2), the strongest contribution to this branch, beginning in February, comes from air masses transported from the subtropics into the polar regions. O_3 loss in these air masses starts in mid-December in the subtropics around 800 (~30 km) and, in the following, moves poleward, descends diabatically to about 550 K (~22 km) and strongly amplifies. At 600 K (~25 km), this signature becomes obvious outside the vortex after the major warming in January (Figure 3, top). In particular, in the mixing zone, i.e., in the region between the vortex edge and the black line confining air masses with more than 5% vortex air (CLaMS vortex tracer), O_3 loss extends well up to the subtropical transport barrier. The highest O_3 loss of about 3 ppmv at 600 K (~25 km) was found at the end of April poleward of 60°N equivalent latitude with relative values of ΔO_3 of up to ≈50%.

[24] Whereas the quality of tracers transported with CLaMS on a time scale of several months in particular their spatial variability strongly depends on the chosen mixing parameters [*Konopka et al.*, 2004], there is a weaker influence of mixing parameters on the pattern of the zonally averaged distributions [*Konopka et al.*, 2003]. Generally, too strong mixing, e.g., brought about by increasing the horizontal resolution from 50 to 200 km, leads to an underestimate of the local ozone loss within the vortex core at 450 K and in the mixing zone at 600 K by about 50%. This is because excessive mixing dilutes too strongly the flux of high pO_3 values both downward within the vortex and from the subtropics into the high latitudes. Thus too strong mixing in the model destroys the reference distribution of pO_3 and, consequently, leads to an underestimate of the halogen- and NO_x-induced contributions to ΔO_3, respectively.

3. Subtropical Versus Mesospheric Sources of NO_x

[25] Air masses within the vortex may also contain large amounts of NO_x, in particular if they have descended from the mesosphere, even in the absence of solar flares. Indeed, in this winter clear signatures of mesospheric air masses inside the Arctic polar vortex were observed during balloon flights of the SPIRALE [*Moreau et al.*, 2005], BONBON [*Schmidt et al.*, 1987] and MIPAS-B [*Friedl-Vallon et al.*, 2004] instruments on 27 January and 6 and 20 March, respectively. These air masses with unusually high CO (more than 500 ppb), extremely low SF_6, and enhanced NO_y were confined to a layer of air that was cut off from the mesosphere during the minor warming in late December 2002 (note that during the autumn 2002 no significant solar flares were observed in the Northern Hemisphere). Thereafter, this layer descended from about 30 km in late January to 25 km in early March and about 22 km altitude in late March (see bold circles in Figure 2, for the approximate positions of the balloon observations) containing a high fraction of mesospheric air [*Engel et al.*, 2006; *Huret et al.*, 2006].

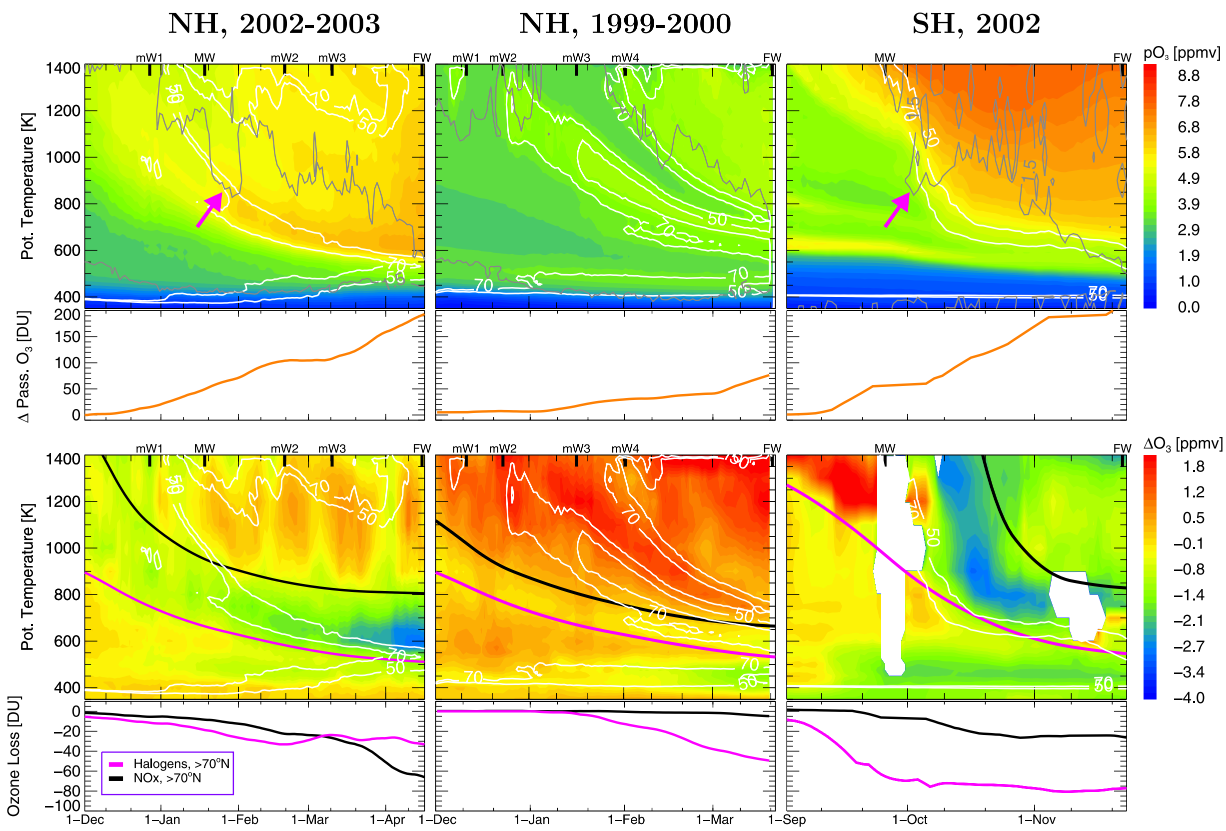

Figure 5. (top) Passive ozone and (bottom) O_3 loss (as discussed in Figure 2) derived from the difference between POAM observations and CLaMS pO_3 for two periods in the Northern Hemisphere (NH): (left) 2002–2003, (middle) 1999–2000 and (right) one period in the Southern Hemisphere (SH) extending over the split event in September 2002. In white regions, in particular for a strongly disturbed vortex after the split event, too few POAM profiles were available. For more detailed explanation see text.

[26] These findings are further supported by the IMK-IAA-MIPAS satellite observations shown in Figure 4. In particular, CO profiles poleward of 70°N equivalent latitude (Figure 4, top) show a clear signature of a disturbance that starts around the end of December in the mesosphere (above 2000 K) and descends to about 800 K (∼30 km) in early January. Afterward, although this signature weakens, the remnants of mesospheric air can be clearly seen until the end of March down to 600 K (∼25 km), i.e., in rough agreement with the balloon observations.

[27] While CO marks mesospheric air, enhanced values of CH_4 indicate extra vortex air transported into the polar region. Such air masses were observed in February and March below 1000 K (∼35 km, Figure 4 (middle)) with substantially increasing CH_4 values starting at the beginning of March. Owing to the complementary information deduced from distributions of CO and CH_4, we can trace the enhanced values of NO_x (Figure 4, bottom) back to either mesospheric sources (enhanced CO) or to air masses transported from low latitudes (enhanced CH_4). Note that because of photochemistry during downward and poleward transport only a limited correlation between NO_x and tracers can be expected. Thus, starting from the end of February, the bulk contribution to the NO_x-related branch of O_3 loss occurs within air masses originating in the subtropics whereas transport from the mesospheric intrusion likewise containing enhanced values of NO_y makes a smaller contribution.

[28] The predominance of the NO_x-induced O_3 loss within the air masses transported to the polar regions over the effect of halogens and the influence of the mesospheric intrusion can also be seen in Figure 2 (bottom) where the calculation of the accumulated column O_3 loss was extended from 65 to 45°N equivalent latitude (pink and black dotted lines). This enlargement of the averaging area by about a factor of 3 decreases the corresponding halogen-induced O_3 loss (solid versus dotted pink line) by approximately the same factor, in particular before the final warming when the halogen-induced O_3 loss is confined by the vortex. On the other hand, the effect of NO_x-induced O_3 loss (more than 80 DU at the beginning of June) hardly depends on the chosen averaging area indicating that NO_x-induced O_3 loss occurs both in high latitudes and in midlatitudes. This further supports our conclusion that horizontal transport of NO_x from the subtropics rather than the descent of NO_x-rich air masses from the mesosphere caused the substantial O_3 loss even if the relative contribution of these two effects cannot be quantified

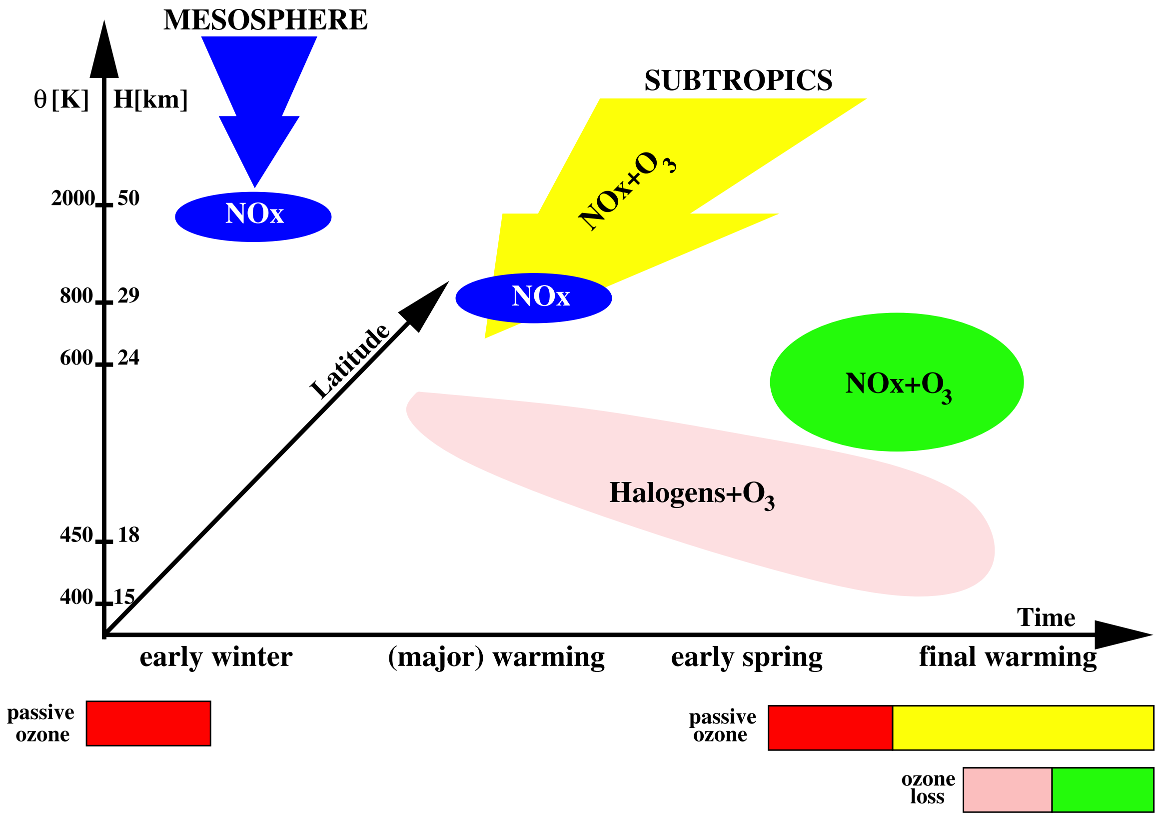

Figure 6. Halogen- versus NO_x-induced O_3 loss. Typically, the halogen-induced O_3 loss in the winter stratosphere occurs within the lower part of the polar vortex that descends during the winter and spring from about 25 to 15 km (light pink). Additionally, during the 2002–2003 period, a strong NO_x-induced O_3 loss could be diagnosed in the polar stratosphere. This branch of O_3 loss was mainly driven by NO_x transported from the subtropics (yellow arrow) after the (wave-2) major warming in January and, to some extent, by the mesospheric air trapped in the vortex at the beginning of the winter (blue). The highest values of O_3 loss were found in the mixing zone above the decaying vortex (green). Beginning in March, the contribution of these air masses to the column O_3 loss accumulated during the winter outweighs the effect of halogens. The lengths of the horizontal bars quantify the column passive O_3 in early winter (left, red) and shortly before the final warming (right, red + yellow). The lengths of the green and light pink bars quantifies the loss processes due to NO_x and halogens, respectively. The column O_3 loss due to NO_x (green) is larger than that due to halogens (light pink) even if the transport of ozone-rich air masses from the subtropics (yellow) counterbalances the loss processes (green + light pink).

exactly (mainly because of insufficient information on the spatial and temporal extension of the mesospheric intrusion).

4. Comparison With 1999–2000 Arctic Winter and the Antarctic Vortex Split Event in 2002

[29] We now discuss whether our findings suggesting that the contribution of the NO_x-induced O_3 loss may dominate the stratospheric O_3 column deficit (i.e., with respect to the pO_3 column) at the end of winter and in early spring can be considered typical. Using the same averaging procedure as in Figure 2, in Figure 5 we compare mean profiles of pO_3 and ΔO_3 poleward of 70°N (note that in Figure 2 the value 65°N was used) for the 2002–2003 period (left column), with a less disturbed Arctic vortex during the 1999–2000 winter [*Newman et al.*, 2002] (middle column) and with a strongly disturbed Antarctic stratosphere in 2002 (right column) when in late September the polar vortex was split into two parts due a major stratospheric warming [*Charlton et al.*, 2004; *Manney et al.*, 2004]. The white contours in Figure 5 are the isolines of the vortex tracer averaged poleward of 70°N and plotted for 50 and 70%. These isolines separate the well-isolated vortex from the midlatitude air. The gray line in Figure 5 (top) quantifies the dynamical permeability of the vortex with the pink arrow denoting a weakening of the transport barrier at the vortex edge after the major warmings [*Steinhorst et al.*, 2005]. All the periods considered extend up to the respective final warmings (FW). Dates for minor (mW) and major (MW) warmings are marked.

[30] The CLaMS simulations, in particular the initialization procedure and the treatment of the boundary conditions are slightly different for all three cases with details described by *Konopka et al.* [2004] and *Konopka et al.* [2005] for the 1999–2000 Arctic period and the Antarctic vortex split period 2002, respectively. Nevertheless, we

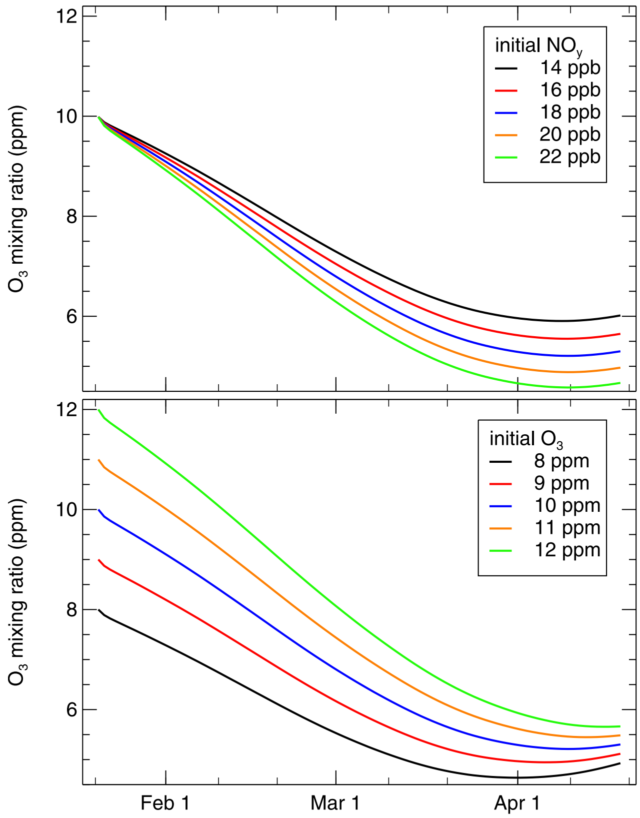

Figure 7. Time series of O_3 moving toward its local equilibrium as derived from box model calculations along an idealized trajectory starting at the end of January in the tropical middle stratosphere at 900 K and instantly shifted at 60°N at 700 K. In this way, we approximate the rapid poleward transport of subtropical air after the major warming in 2002. The model was initialized from the HALOE climatology and the Mainz-2D model. (top) Sensitivity of the NO_x-induced ozone loss to the initial value of NO_y in the box. (bottom) Sensitivity to the initial value of O_3 for a constant NO_y value of 18 ppbv.

believe that all three simulations are robust enough to describe the quantitative differences in the patterns of O_3 loss.

[31] First, in the upper two rows of Figure 5 we compare the differences in the distribution of pO_3 caused by different planetary wave forcing and strengths of the vortex edge. Whereas during the 2002–2003 period, a deep intrusion of subtropical O_3 triggered by the major warming around mid-January 2002 (thick pink arrow) determines the values of pO_3 above 800 K (≈7 ppmv), the lack of major warmings during 1999–2000 leads to a vertically more uniform pO_3 distribution for the same season and region (the highest values of pO_3 do not exceed 5 ppmv). In contrast to the 1999–2000 period, which represents a only weakly distributed vortex, the Antarctic split period in 2002 shows more similarities with the 2002–2003 period in the Arctic. In particular, the major warming in September 2002 completely destroyed the upper part of the vortex and the subsequent intrusion of the subtropical air increased the mean values of pO_3 to about 9 ppmv. Whereas during the 2002–2003 period, the strongest poleward flux of high O_3 values occurred at ~800 K, the highest values of pO_3 after the Antarctic vortex split in 2002 were localized above 1000 K. The time dependence of the column of pO_3 integrated between 350 and 1400 K (second row in Figure 5) shows how increased poleward transport of O_3 significantly enhanced the (mean) column of the polar pO_3 after the major warmings in 2003 (Arctic) and 2002 (Antarctic) whereas only a small increase of pO_3 could be diagnosed for the 1999–2000 period.

[32] The bottom two rows in Figure 5 show the corresponding O_3 loss diagnosed from the difference between the POAM observations and CLaMS pO_3 The halogen-induced O_3 losses (in the region below the thick pink line) show similar signatures for the Arctic periods 2002–2003 and 1999–2000 with mean column loss up to about 40 DU around the end of March (pink lines in the lowest row of Figure 5) whereas ΔO_3 within the Antarctic vortex is approximately twice as large shortly before the vortex split. The time dependence and the magnitude of the column O_3 loss agree fairly well with the results of *Harris et al.* [2002], *Tilmes et al.* [2003] and *Randall et al.* [2004], for all three periods, respectively, although the results compared are based on different diagnostics and averaging procedures.

[33] The main focus of this paper is NO_x-induced O_3 loss, i.e., the O_3 deficit diagnosed in the regions roughly confined by the thick pink and black lines in the third row of Figure 5 (the black lines for the Arctic periods 2002–2003 and 1999–2000 are chosen in such a way that the strongest signal of NO_x-induced ΔO_3 is contained between the black and pink lines. The column O_3 losses due to NO_x (black lines in the bottom row of Figure 5) for both the Arctic 2002–2003 and the Antarctic 2002 split period continuously increase after the major warmings in January and September in the Northern and Southern hemispheres, respectively. The smaller impact on column ΔO_3 during the Antarctic split period is due to an altitude of the subtropical intrusion, which is higher by ≈100 K, i.e., by a smaller density of O_3 within the subtropical intrusion. This is also the reason why the exact positions of the black lines do not influence the inferred numbers of the column ΔO_3. Furthermore, comparison between Figure 5 and Figure 2 where POAM profiles with equivalent latitude <70° and 65°N, respectively, were averaged, shows the same patterns of ΔO_3 and negligible differences of inferred column ΔO_3.

[34] From a dynamical point of view, the increased poleward transport during these two periods was triggered by major warmings associated with strong planetary wave-2 activities splitting the midstratospheric polar vortex [*Kleinböhl et al.*, 2005; *Manney et al.*, 2004]. Thus, similar to the case of the low-O_3 pockets [*Morris et al.*, 1998], air masses from low latitudes are transported to polar regions where, because of reduced solar exposure, O_3 production is suppressed and, consequently, O_3 loss occurs establishing a new local photochemical equilibrium [see also *Kawa et al.*, 2002]. Idealized box model calculations show (next section) that this effect is mainly determined by the poleward transport rather than by descent outside of the polar vortex. Whereas the low-O_3 pockets describe air masses which are trapped within the polar anticyclones formed during a wave-1 event and which can be transported

back into the midlatitudes, the wave-2 pattern increases more effectively the irreversible poleward transport of O_3 [*Nathan et al.*, 2000].

5. Discussion and Conclusions

[35] The spatial and temporal course of events during the 2002–2003 period in the Arctic is schematically summarized in Figure 6. Triggered by the minor warming in late December 2002 and the major warming in January 2003 (wave-2 event), the NO_x-rich layer (blue) was separated from the mesosphere and descended into the polar vortex. Additionally, driven by these warmings, O_3- and NO_x-rich subtropical air was transported from the subtropical middle stratosphere into the polar region (yellow). In these air masses, a substantial NO_x-induced O_3 loss occurred that continued during the following period when subtropical air masses were mixed with the vortex air through a weak and permeable vortex edge (green).

[36] Consequently, the passive O_3 (red) increased (yellow) and the loss processes responsible for column ozone loss in polar latitudes can be divided into the halogen-induced contribution within the polar vortex (light pink) and the NO_x-induced contribution in air masses transported from the subtropics and mixed across a weak polar vortex edge into the polar stratosphere, roughly above the region affected by the halogens (green). Thus, shortly before the final warming in mid-April 2003, the NO_x-induced O_3 loss outweighed the effect of the halogens on column O_3, although the 2002–2003 period is not one of the winters with low, but with rather moderate, halogen-induced O_3 loss compared to other Arctic winters between 1991 and 2003 [*Tilmes et al.*, 2004]. It is also noteworthy that such overlying O_3 loss processes as reported here may complicate the interpretation of the total O_3 column observations, in particular, by attributing trends derived from such observations to a particular chemical mechanism.

[37] It should be emphasized that despite the described O_3 loss processes due to halogens and NO_x-related chemistry around and after the major warmings in 2002 and 2003, the transport of O_3-rich air masses from the tropics counterbalanced the loss processes. In particular, the mean total O_3 increased by at least 80 DU poleward of 70° equivalent latitude around the end of both periods, as can be derived from a comparison of the second and fourth row in Figure 5. Thus, despite the substantial ozone loss, the net balance after the major warmings is positive; that is, O_3 increase due to poleward transport of high subtropical values outweighs the ozone loss processes.

[38] Nevertheless, because of a high NO_y content in these air masses, the question arises of whether enhanced values of NO_y, which are transported rapidly from the subtropics into high latitudes, can destroy so much O_3 that the resulting mixing ratios are below the expected climatological values. We discuss this question by using an idealized box model where a parcel with a composition typical of the middle stratosphere in the subtropics adjusts its chemical equilibrium to late spring conditions in the polar stratosphere. In the PSC-free polar stratosphere, between $\theta = 600$ and 900 K, the major catalytic cycle destroying ozone is the NO-NO_2 cycle [*Crutzen*, 1970] with the rate-limiting reaction between NO_2 and O and with a relative contribution of 76% according to our box model calculations. The contributions of the other cycles, driven by OH, O, Cl, and Br [*Dessler*, 2000], are given by 12.5, 7, 3.5, and 1%, respectively.

[39] In Figure 7, the results along an idealized air mass trajectory are shown. Along these trajectories high values of O_3 and NO_y are transported, without mixing, from low to high latitudes. The model is initialized at the end of January at 900 K by using the HALOE climatology and the Mainz-2D model [*Grooß*, 1996; *Grooß and Russell*, 2005]. Then, to estimate the effect of a rapid poleward transport due to the major warming as discussed in this paper for the 2002–2003 Arctic period, we instantly shift the considered box from the tropics to 60°N and 700 K and discuss how, mainly because of NO_x chemistry, the O_3 value within the box moves toward its local chemical equilibrium [*Morris et al.*, 1998].

[40] As can be seen in Figure 7 (top), this equilibrium is reached around the beginning of April with values of O_3 between 4 and 6 ppmv, derived by varying the initial NO_y loading between 22 and 14 ppbv, respectively (based on 2D model studies, *Dessler* [2000] suggests values up 24 ppbv whereas NO_x values around 17 ppbv can be found in the HALOE climatology [*Grooß and Russell*, 2005]). Figure 7 (bottom) shows that after adjusting its local equilibrium O_3 in the box depends only weakly on its initial value at the beginning of the simulation (here calculated for 18 ppb NO_y). Thus O_3 within the box in high latitudes is mainly controlled by the amount of NO_y transported from the subtropics with a minor dependence on the initial value of O_3. Thus the O_3 volume mixing ratio in late spring can be reduced below its expected climatological value of around 5 ppmv according to the HALOE climatology [*Grooß and Russell*, 2005].

[41] We conclude that an increased poleward transport of NO_y in the midstratosphere, as assumed here in idealized box model calculations, has the potential to enhance the amount of NO_x in high latitudes and, consequently, to reduce the column O_3 below climatological values, in particular during summer when high-latitude column O_3 is controlled by catalytic cycles driven by NO_x. In the future, this scenario of O_3 depletion in the polar stratosphere may become more typical if, as predicted by climate models [*Austin et al.*, 2003; *Schnadt and Dameris*, 2003], the effect of halogens decreases and the climate change forces a "dynamically more active" stratosphere with increased transport from the subtropics and the mesosphere into the polar regions.

[42] Furthermore, the positive trend of N_2O (0.75 ppbv/year since the late 1970s [*WMO*, 2003]), that is of the main source of NO_y in the middle stratosphere, will lead to an increase in the stratospheric NO_y loading during the next decades. By assuming that about 320 ppbv N_2O correspond to about 20 ppbv NO_y loading in the lower stratosphere, the extrapolation of the current N_2O trends into the future (0.75 ppbv/year) leads to an estimated increase of NO_y loading by 1 ppbv in the next 21 years. It should be emphasized that to confirm our speculation on the role of NO_x in the future (our results for disturbed winters show an increase rather than a decrease of total O_3 column) requires full chemistry studies over all seasons with

appropriate NO_y sources and with enhanced meridional transport.

[43] **Acknowledgments.** We thank three anonymous reviewers for their very constructive remarks. The European Centre for Medium-Range Weather Forecasts (ECMWF) is acknowledged for meteorological data support. This study has been partly supported by the German Research Foundation (DFG) under grant KO 2958/1-1 within the SPP 1176 "CAWSES–Climate And Weather of the Sun-Earth System."

References

Austin, J., et al. (2003), Uncertainties and assessments of chemistry-climate models of the stratosphere, *Atmos. Chem. Phys.*, *3*, 1–27.

Brasseur, G., and S. Solomon (1984), *Aeronomy of the Middle Atmosphere*, Springer, New York.

Charlton, A. J., A. O'Neill, W. A. Lahoz, and P. Berrisford (2004), The splitting of the stratospheric polar vortex in the Southern Hemisphere, September 2002: Dynamical evolution, *J. Atmos. Sci.*, *62*, 590–602.

Crutzen, P. J. (1970), The influence of nitrogen oxides on the atmospheric ozone content, *Q. J. R. Meteorol. Soc.*, *96*, 320–325.

Dessler, A. E. (2000), *The Chemistry and Physics of Stratospheric Ozone*, *Int. Geophys. Ser.*, vol. 74, edited by R. Dmowska, J. R. Holton, and H. T. Rossby, 214 pp., Elsevier, New York.

Engel, A., et al. (2006), On the observation of mesospheric air inside the arctic stratospheric polar vortex in early 2003, *Atmos. Chem. Phys.*, *6*, 267–282.

European Space Agency (2000), Envisat, MIPAS: An instrument for atmospheric chemistry and climate research, *ESA Spec. Publ., SP-1229*.

Fahey, D. W., and A. R. Ravishankara (1999), Summer in the stratosphere, *Science*, *285*, 208–210.

Farman, J. C. (1985), Ozone photochemistry in the Antarctic stratosphere in summer, *Q. J. R. Meteorol. Soc.*, *111*, 1013–1025.

Feng, W., et al. (2005), Three-dimensional model study of the Arctic ozone loss in 2002/2003 and comparison with 1999/2000 and 2003/2004, *Atmos. Chem. Phys.*, *5*, 139–152.

Friedl-Vallon, F., G. Maucher, A. Kleinert, A. Lengel, C. Keim, H. Oelhaf, H. Fischer, M. Seefeldner, and O. Trieschmann (2004), Design and characterization of the balloon-borne Michelson Interferometer for Passive Atmospheric Sounding (MIPAS-B2), *Appl. Opt.*, *43*, 3335–3355.

Funke, B., et al. (2004), Retrieval of stratospheric NO_x from 5.3 and 6.2 μm nonlocal thermodynamic equilibrium emissions measured by Michelson Interferometer for Passive Atmospheric Sounding (MIPAS) on Envisat, *J. Geophys. Res.*, *110*, D09302, doi:10.1029/2004JD005225.

Glatthor, N., et al. (2004), Spaceborne ClO observations by the Michelson Interferometer for Passive Atmospheric Sounding (MIPAS) before and during the Antarctic major warming in September/October 2002, *J. Geophys. Res.*, *109*, D11307, doi:10.1029/2003JD004440.

Grooß, J.-U. (1996), Modelling of stratospheric chemistry based on HALOE/UARS satellite data, Ph.D. thesis, Univ. of Mainz, Mainz, Germany.

Grooß, J.-U., and J. M. Russell (2005), Technical note: A stratospheric climatology for O_3, H_2O, CH_4, NO_x, HCL, and HF derived from HALOE measurements, *Atmos. Chem. Phys.*, *5*, 2797–2807.

Grooß, J.-U., G. Günther, R. Müller, P. Konopka, S. Bausch, H. Schlager, C. Voigt, C. M. Volk, and G. C. Toon (2005), Simulation of denitrification and ozone loss for the Arctic winter 2002/2003, *Atmos. Chem. Phys.*, *5*, 2973–2988.

Harris, N. R., M. Rex, F. Goutail, B. M. Knudsen, G. L. Manney, R. Müller, and P. von der Gathen (2002), Comparison of empirically derived ozone loss rates in the Arctic vortex, *J. Geophys. Res.*, *107*(D20), 8264, doi:10.1029/2001JD000482.

Huret, N., M. Pirre, A. Hauchecorne, C. Robert, and V. Catoire (2006), On the vertical structure of the stratosphere at mid-latitude during the first stage of the polar vortex formation and in the polar region in the presence of a large mesospheric descent, *J. Geophys. Res.*, *111*, D06111, doi:10.1029/2005JD006102.

Kawa, S. R., R. M. Bevilacqua, J. J. Margitan, A. R. Douglass, M. R. Schoeberl, K. W. Hoppel, and B. Sen (2002), Interaction between dynamics and chemistry of ozone in the setup phase of the Northern Hemisphere polar vortex, *J. Geophys. Res.*, *107*, 8310, doi:10.1029/2001JD001527, [printed 108(D5), 2003].

Kleinböhl, A., J. Kuttippurath, M. Sinnhuber, B. M. Sinnhuber, H. Küllmann, K. F. Künzi, and J. Notholt (2005), Rapid meridional transport of tropical airmasses to the Arctic during the major stratospheric warming in January 2003, *Atmos. Chem. Phys.*, *5*, 1291–1299.

Konopka, P., J. U. Grooß, G. Günther, D. S. McKenna, R. Müller, J. W. Elkins, D. Fahey, and P. Popp (2003), Weak impact of mixing on chlorine deactivation during SOLVE/THESEO2000: Lagrangian modeling (CLaMS) versus ER-2 in situ observations, *J. Geophys. Res.*, *108*(D5), 8324, doi:10.1029/2001JD000876.

Konopka, P., et al. (2004), Mixing and ozone loss in the 1999–2000 Arctic vortex: Simulations with the 3-dimensional Chemical Lagrangian Model of the Stratosphere (CLaMS), *J. Geophys. Res.*, *109*, D02315, doi:10.1029/2003JD003792.

Konopka, P., J.-U. Grooß, K. Hoppel, H.-M. Steinhorst, and R. Müller (2005), Mixing and chemical ozone loss during and after the Antarctic polar vortex major warming in September 2002, *J. Atmos. Sci.*, *62*(3), 848–859.

Lait, L. R. (1994), An alternative form for potential vorticity, *J. Atmos. Sci.*, *51*, 1754–1759.

López-Puertas, M., et al. (2005), HNO_3, N_2O_5 and $ClONO_2$ enhancements after the October-November 2003 solar proton events, *J. Geophys. Res.*, *110*, A09S44, doi:10.1029/2005JA011051.

Lucke, R. L., et al. (1999), The Polar Ozone and Aerosol Measurement (POAM) III instrument and early validation results, *J. Geophys. Res.*, *104*, 18,785–18,799.

Lumpe, J. D., R. M. Bevilacqua, K. W. Hoppel, and C. E. Randell (2002), POAM III retrieval algorithm and error analysis, *J. Geophys. Res.*, *107*(D21), 4575, doi:10.1029/2002JD002137.

Manney, G. L., R. W. Zurek, A. O'Neill, and R. Swinbank (1994), On the motion of air through the stratospheric polar vortex, *J. Atmos. Sci.*, *51*, 2973–2994.

Manney, G. L., L. Froidevaux, M. L. Santee, N. J. Livesey, J. L. Sabutis, and J. W. Waters (2003), Variability of ozone loss during Arctic winter (1991 to 2000) estimated from UARS Microwave Limb Sounder measurements, *J. Geophys. Res.*, *108*(D4), 4149, doi:10.1029/2002JD002634.

Manney, G. L., J. L. Sabitus, D. R. Allen, W. A. Lahoz, A. A. Scaife, C. E. Randell, S. Pawson, B. Naujokat, and R. Swinbank (2004), Simulations of dynamics and transport during the September 2002 Antarctic major warming, *J. Atmos. Sci.*, *37*(66), 1151–1157.

McKenna, D. S., P. Konopka, J.-U. Grooß, G. Günther, R. Müller, R. Spang, D. Offermann, and Y. Orsolini (2002), A new Chemical Lagrangian Model of the Stratosphere (CLaMS): 1. Formulation of advection and mixing, *J. Geophys. Res.*, *107*(D16), 4309, doi:10.1029/2000JD000114.

Moreau, G., C. Robert, V. Catoire, C. Camy-Perret, N. Huret, M. Pirre, L. Pomathiod, and M. Chartier (2005), SPIRALE: A multispecies in situ balloon-borne instrument with six tunable diode laser spectrometers, *Appl. Opt.*, *44*(28), 5972–5989.

Morris, G. A., S. R. Kawa, A. R. Douglass, M. R. Schoeberl, L. Froidevaux, and J. Waters (1998), Low-ozone pockets explained, *J. Geophys. Res.*, *103*, 3599–3610.

Nash, E. R., P. A. Newman, J. E. Rosenfield, and M. R. Schoeberl (1996), An objective determination of the polar vortex using Ertel's potential vorticity, *J. Geophys. Res.*, *101*, 9471–9478.

Natarajan, M., E. E. Remsberg, and L. E. Deaver (2004), Anomalously high levels of NO_x in the polar upper stratosphere during April, 2004: Photochemical consistency of HALOE observations, *Geophys. Res. Lett.*, *31*, L15113, doi:10.1029/2004GL020566.

Nathan, T. R., E. C. Cordero, L. Long, and D. Wuebbles (2000), Effects of planetary wave-breaking on the seasonal variation of total column ozone, *Geophys. Res. Lett.*, *27*, 1907–1910.

Newman, P. A., D. W. Fahey, W. B. Brune, and M. J. Kurylo (1999), Preface to POLARIS special section, *J. Geophys. Res.*, *104*(D21), 26,481–26,495.

Newman, P. A., et al. (2002), An overview of the SOLVE/THESEO 2000 campaign, *J. Geophys. Res.*, *107*(D20), 8259, doi:10.1029/2001JD001303.

Perliski, L. M., S. Solomon, and J. London (1989), On the interpretation of seasonal-variations of stratospheric ozone, *Planet. Space Sci.*, *37*, 1527–1538.

Randall, C. A., G. L. Manney, D. R. Allen, R. M. Bevilacqua, J. Hornstein, C. Trepte, W. Lahoz, J. Ajtic, and G. Bodeker (2004), Reconstruction and simulation of stratospheric ozone distributions during the 2002 Austral winter, *J. Atmos. Sci.*, *62*(14), 748–764.

Schmidt, U., G. Kulessa, E. Klein, E.-P. Röth, P. Fabian, and R. Borchers (1987), Intercomparison of balloon-borne cryogenic whole air samplers during the MAP/GLOBUS 1983 campaign, *Planet. Space Sci.*, *35*, 647–656.

Schnadt, C., and M. Dameris (2003), Relationship between North Atlantic Oscillation changes and stratospheric ozone recovery in the Northern Hemisphere in a chemistry-climate model, *Geophys. Res. Lett.*, *30*(9), 1487, doi:10.1029/2003GL017006.

Singleton, C. G., et al. (2005), 2002–2003 Arctic ozone loss deduced from POAM III satellite observations and the SLIMCAT chemical transport model, *Atmos. Chem. Phys.*, *5*, 597–609.

Siskind, D. E., G. E. Nedoluha, C. E. Randall, M. Fromm, and J. M. Russell III (2000), An assessment of Southern Hemisphere stratospheric NO_x enhancements due to transport from the upper atmosphere, *Geophys. Res. Lett.*, *27*(3), 329–332.

Solomon, S. (1999), Stratospheric ozone depletion: A review of concepts and history, *Rev. Geophys.*, *37*(3), 275–316.

Steinhorst, H.-M., P. Konopka, G. Günther, and R. Müller (2005), How permeable is the edge of the Arctic vortex: Model studies of the winter 1999–2000, *J. Geophys. Res.*, *110*, D06105, doi:10.1029/2004JD005268.

Tilmes, S., R. Müller, J.-U. Grooß, M. Höpfner, G. C. Toon, and J. M. Russell (2003), Very early chlorine activation and ozone loss in the Arctic winter 2002–2003, *Geophys. Res. Lett.*, *30*(23), 2201, doi:10.1029/2003GL018079.

Tilmes, S., R. Müller, J.-U. Grooß, and J. M. Russell (2004), Ozone loss and chlorine activation in the Arctic winters 1991–2003 derived with the tracer-tracer correlations, *Atmos. Chem. Phys.*, *4*(8), 2181–2213.

von Clarmann, T., et al. (2005), Experimental evidence of perturbed odd hydrogen and chlorine chemistry after the October 2003 solar proton events, *J. Geophys. Res.*, *110*, A09S45, doi:10.1029/2005JA011053.

World Meteorological Organization (2003), Scientific assessment of ozone depletion: 2002, *Rep. 47*, Geneva, Switzerland.

A. Engel and T. Wetter, Institut für Meteorologie und Geophysik, Johann Wolfgang Goethe-Universität Frankfurt, D-60325 Frankfurt am Main, Germany.

B. Funke and M. López-Puertas, Instituto de Astrofisica de Andalucia, Consejo Superior de Investigaciones Cientficas, E-18080 Granada, Spain.

N. Glatthor, H. Oelhaf, G. Stiller, T. von Clarmann, and G. Wetzel, Institut für Meteorologie und Klimaforschung, Forschungszentrum Karlsruhe, D-76021 Karlsruhe, Germany.

J.-U. Grooß, G. Günther, P. Konopka, R. Müller, and M. Riese, Forschungszentrum Jülich, ICG-I, Forschungszentrum Jülich, D-52425 Jülich, Germany. (p.konopka@fz-juelich.de)

N. Huret and M. Pirre, Laboratoire de Physique et Chemie de l'Environnement, F-45071 Orleans, France.